Ligand Diffusion, Receptor Binding, and Internalization: Zeroth-Order Kinetics

William Strieder
Dept. of Chemical Engineering, University of Notre Dame, Notre Dame, IN 46556

The exact, analytical solution for steady-state diffusion and zeroth-order surface reaction at a cell-wall chemoreceptor site is presented. Following Berg (1993), and others, the receptor is modeled as a chemically active circular site on an impermeable, inert cell wall. Explicit values of the dimensionless site-specific rate constant mark the regions of chemical-, transitional- and diffusion-controlled kinetics. Particularly when the Michaelis-Menten constant is small relative to the ligand bulk concentration, this simple form of the receptor-site reaction current should provide a useful model for cell growth-factor internalization, nutrient uptake, and certain cellular signaling behaviors. Various biophysical conditions that cause site mass-transport resistance in cellular site-reaction kinetic processes are discussed.

Introduction

The interaction of ligand diffusion and ligand–receptor surface reactions at cell receptor sites can be a significant step in cellular behavior processes. To determine the ligand-site diffusion resistance, the cell-wall site geometry must be specified. Berg and Purcell (1977) have modeled the receptor site as a reactive disk of radius a embedded in a smooth impermeable, inert cell-wall surface. Koren and Hammes (1976) state that due to steric effects, only 2% of the solid angle of approach to a ligand receptor leads to reaction. In most of the previous work on the disk-site model (Berg and Purcell, 1977; Berg and von Hippel, 1985; Northrup, 1988; Zwanzig, 1990; Berg, 1993), the sites were assumed to be infinitely reactive, the reaction was diffusion limited with a ligand diffusion coefficient D, and the reaction current R_∞ into the site for this case is given by

$$R_\infty = 4aD\,c_0, \tag{1}$$

where c_0 is the uniform reactant concentration far from the site. In this limit the ligand concentration vanishes across the active site, but the local flux must vary to a minimum value at the site center. But Lauffenburger and Linderman (1993) have pointed out that, while some diffusion-controlled receptors exist, many are not this reactive, and a combination of finite surface reaction and local diffusion resistance to the site is more common.

Extracellular ligand diffusion to a chemoreceptor bound within the cell wall, association–dissociation reactions at the receptor's active site to form a complex, and subsequent consumption by the cell are often the initial steps in a complex set of ordered biophysiochemical events that determine cellular communication and growth. When the internalization is represented by a forward rate constant (Lauffenburger and Linderman, 1993; Hoffman et al., 1996), and when steady-state (or pseudo-steady-state) conditions exist in the cell wall (Wiley and Cunningham, 1981), the overall site kinetics for ligand uptake into the cell is Michaelis-Menten. In addition, the association reaction is sometimes very rapid, leading to ligand saturation of the receptor sites, and cell-wall-site kinetics become zeroth-order in ligand concentration c

$$r_m = \sigma, \qquad 0 < c(r), \qquad (r \text{ on the site}) \tag{2a}$$

pointwise at each site point r per unit area of active site surface. Note that in contrast to the diffusion-controlled case of Eq. 1, here the local site flux is constant, while the local ligand concentration varies pointwise across the site to a minimum value at the site center.

But Eqs. 1 and 2a do not cover all cases. When the diffusion resistivity is large or if the external ligand concentration c_0 is small, the ligand flux at an infinitesimal area element of the site can fall below σ. The ligand concentration falls to zero at this site point:

$$0 < r_m < \sigma, \qquad c(r) = 0, \qquad (r \text{ on the site}). \tag{2b}$$

In this case the local diffusive flux to the site surface-area element at r sets the ligand consumption rate, that is, local diffusion control. As mentioned previously, a ligand flux distribution can occur radially across the site. For certain intermediate σ values, the outer ring of the site has a sufficient flux to maintain σ, that is, Eq. 2a, whereas toward the center diffusion-limited conditions with the corresponding zero local site ligand concentration exists, that is, Eq. 2b. Of course, with increasing σ values of surface reactivity, the site eventually becomes completely diffusion controlled and the conditions for Eq. 1, a diffusion-controlled site reaction, is reached. Equations 2a and 2b are the mathematical limit of Michaelis-Menten kinetics, when the denominator coefficient is much smaller than the bulk ligand concentration c_0.

Examples of zeroth-order ligand consumption kinetics at the cell-wall receptor site can be found in the monograph of Lauffenburger and Linderman (1993). For one case in particular, they have proposed zeroth-order site kinetics for the process of desensitization during cellular signal transduction. Wiley and Cunningham (1981) have shown that Michaelis-Menten kinetics is appropriate for analyzing cellular site binding and internalization of epidermal growth factor in human fibroblasts. But their measured Michaelis-Menten denominator value is so small ($=5.62\times10^{-10}$ molar) that the reaction is essentially zeroth order, even at very low ligand concentrations. In their discussion of nutrient utilization and Monod kinetics for cell growth, Bailey and Ollis (1986) note that the Monod kinetics denominator constant is quite often rather small (and unknown). While they do not attempt a molecular explanation, the Monod nutrient uptake kinetic form does suggest the application of these considerations to nutrient uptake during cell growth. Finally, for strong reactant adsorption, zeroth-order site kinetics is appropriate for gas–solid reactions (Maalmi et al., 1995) with nonuniform surfaces, as well as active catalyst centers or microcrystals on an inert support for heterogeneous catalysis.

To our knowledge, little has been done for finite site reaction kinetics (Strieder, 1999), and the practice in recent literature (Lauffenburger and Linderman, 1993) is to add the diffusion-control and chemical-reaction-control limits in series

$$R_{\mathrm{apx}}/R_{\infty}=\Psi\,(\Psi+4/\pi)^{-1}, \tag{3}$$

where Ψ is the dimensionless specific reaction rate

$$\Psi=(a\sigma)/(c_0 D). \tag{4}$$

This approach bypasses the fundamental analysis of the circular site diffusion-reaction problem, and gives little insight into the underlying local diffusion fluxes and reaction rates. It is quite reasonable to argue that the exact solution of the zeroth-order site reaction-diffusion problem will provide a more useful extimate than series additivity (Eqs. 3–4). The purpose of this article is to develop and discuss the exact, analytical solution for the steady-state diffusion to, and zeroth-order surface reaction within, a circular active site at the center of a large inert plane.

Receptor Model Equations

The receptor on the cell wall surface is modeled (Berg and Purcell, 1977; Berg, 1993; Zwanzig, 1990) as a chemically active disk of radius, a, located at the center of an otherwise impenetrable, inert, nonadsorbing plane. In contact with this surface is a solution containing nutrient or ligand reactant with a local concentration, c. On the circle surface the reaction is zeroth order with a constant, maximum rate σ per unit area. At large distances from the circle's center, the reactant concentration approaches a uniform value c_0. Fickian diffusion with constant coefficient D transports the reactant to the circular active site.

When the origin of cylindrical coordinates is placed at the center of the circular surface site, the reactant concentration c will depend on the radial r and axial z distances from the reactive site center. The concentration is written in terms of the dimensionless dependent variable u,

$$c=c_0(1+u). \tag{5}$$

The substitution simplifies both the derivation and the form of the transformed differential equations. The steady-state diffusion equation expressed in terms of the dimensionless radial ρ and axial ζ coordinates

$$\rho=\mathrm{r}/a, \qquad \zeta=z/a, \tag{6a),(6b}$$

becomes

$$\frac{1}{\rho}\frac{\partial}{\partial\rho}\left(\rho\frac{\partial u}{\partial\rho}\right)+\frac{\partial^2 u}{\partial\zeta^2}=0. \tag{7}$$

Boundary conditions far from the reactive site are

$$u=0\begin{cases}\rho\to\infty, & \text{any } \zeta & \text{(8a)}\\ \zeta\to\infty, & \text{any } \rho, & \text{(8b)}\end{cases}$$

while on the surface outside of the active circular site

$$\frac{\partial u}{\partial\zeta}=0, \qquad \rho>1, \qquad \zeta=0. \tag{9}$$

There are three possible kinetics scenarios within the active site, depending on the value of $\Psi[=a\sigma/(c_0 D)]$defined by Eq. 4. If the dimensionless reaction rate Ψ is very small, the local reactant concentration is uniform across the receptor site. When the rate is increased somewhat, the surface ligand concentration will develop a minimum at the site center, but the local site concentration values will remain positive. If the zeroth-order rate is increased up to a critical value Ψ_c, the central site ligand concentration will drop to zero, Eq. 2a describes the active site surface kinetics at every point on the unit circular site, and the reaction rate current R_0 is $\pi a^2\sigma$:

$$0 < \Psi \le \Psi_c, \tag{10a}$$

$$\frac{\partial u}{\partial \zeta} = \Psi, \qquad \zeta = 0, \qquad 0 < \rho < 1, \tag{10b}$$

$$R_0 = \pi a^2 \sigma. \tag{10c}$$

If the reaction rate Ψ is greater than Ψ_c, but less than the rate value Ψ_∞ necessary for complete diffusion control across the site, a second scenario takes place. A circle, whose dimensionless radius ρ_0 can have a value from zero to one, is drawn on the surface $\zeta = 0$ about the site center. Then the kinetics equation (Eq. 2a) holds for the outside ring of the site, while Eq. 2b for vanishing surface concentration with diffusion control holds within the inner radius ρ_0:

$$\Psi_c < \Psi < \Psi_\infty, \tag{11a}$$

$$\frac{\partial u}{\partial \zeta} = \Psi, \qquad \zeta = 0, \qquad \rho_0 < \rho < 1, \tag{11b}$$

$$1 + u = 0, \qquad \zeta = 0, \qquad 0 < \rho < \rho_0. \tag{11c}$$

If Ψ lies above Ψ_∞, the kinetics equation (Eq. 2b) of zero concentration is applied across the entire site, the site reaction rate is totally diffusion controlled, and the site reaction current R_∞ is given by Eq. 1:

$$\Psi_\infty \le \Psi < \infty, \qquad R = R_\infty. \tag{12}$$

In general the reaction-rate current R into the circular receptor site has the form:

$$R = 2\pi a D c_0 \int_0^1 d\rho\rho \, \partial u/\partial \zeta, \qquad \zeta = 0, \tag{13}$$

where the integration of the reactant flux is over the circular site area.

Hankel Transformation

The Hankel transformation analysis of Eqs. 5–8b is the same for all three kinetics scenarios, Eqs. 10–12. Tranter (1966) has shown that the solution of Eqs. 5–8b can be expressed in terms of the Hankel transformation $\bar{u}$ of u over ρ from zero to infinity:

$$\bar{u}(\xi, \zeta) = \int_0^\infty d\rho\rho \, u(\rho, \zeta) J_0(\xi\rho), \tag{14}$$

where $\xi (0 \le \xi < \infty)$ is the Hankel transform independent variable, and $J_0(\xi\rho)$ is the zeroth-order Bessel function of the first kind (Abramowitz and Stegun, 1965). The transform operation is applied to the differential equation (Eq. 7) and, after integration by parts along with the application of boundary condition (Eq. 8a), it becomes,

$$\frac{\partial^2 \bar{u}}{\partial \zeta^2} - \xi^2 \bar{u} = 0, \tag{15}$$

whose solution with the boundary condition expressed in Eq. 8b has the form

$$\bar{u} = A(\xi) \exp(-\xi\zeta). \tag{16}$$

The inverse Hankel transformation gives the exact solution

$$u = \int_0^\infty d\xi\xi A(\xi) \exp(-\xi\zeta) J_0(\rho\xi), \tag{17}$$

in terms of the Hankel transform coefficient $A(\xi)$. Note that the transform coefficient A cannot depend on ρ or ζ.

The first scenario, $0 < \Psi \le \Psi_c$, of Eqs. 10a—10c is of note because we already know the answer, the site reaction current is given by R_0 of Eq. 10c. But we don't know when to apply R_0, that is, the value of Ψ_c. The experimental significance of Ψ_c comes from the dependence of the site reaction current R on the applied bulk ligand concentration c_0. When the bulk ligand concentration c_0 lies at or above the critical concentration $\sigma a (D\Psi_c)^{-1}$, the ligand reaction current R_0 into the site is independent of the specific c_0 value. For bulk ligand concentrations below $\sigma a (D\Psi_c)^{-1}$ diffusion plays a role, R depends on c_0, and ultimately at sufficiently small values of c_0, R goes to zero with the bulk ligand concentration c_0.

For the kinetic scenario (Eq. 10a), substitution of Eq. 17 into the two boundary conditions (Eqs. 9 and 10b) yields

$$\int_0^\infty d\xi f(\xi) \, J_0(\rho\xi) = 0, \qquad 1 < \rho < \infty, \tag{18}$$

and

$$\int_0^\infty d\xi f(\xi) \, J_0(\rho\xi) = \Psi, \qquad 0 < \rho < 1, \tag{19}$$

where

$$f(\xi) = -\xi^2 A(\xi). \tag{20}$$

Tranter (1966) have given the solution of the dual-coupled integral equations (Eqs. 18–20) as an exercise problem, and

$$f(\xi) = \Psi \, J_1(\xi). \tag{21}$$

Watson (1966) has discussed the dual integrals obtained when Eq. 21 is substituted into Eqs. 18 and 19 and gives these analytical forms.

The reaction concentration profile c, can be obtained across the site surface from the simultaneous use of Eqs. 5, 17, and 21

$$c = c_0 - c_0 \Psi \int_0^\infty d\xi\xi^{-1} J_1(\xi) J_0(\xi\rho), \qquad \zeta = 0. \tag{22}$$

This integral (Eq. 22) of a Bessel function product is listed in Bateman's table (1954) as,

$$c = c_0 - 2c_0 \Psi E(\rho^2)/\pi, \qquad 0 < \rho < 1, \qquad \zeta = 0, \tag{23}$$

where $E(\rho^2)$ is the elliptic function of the second kind. Note that the Bateman (1954) notation $E(\rho)$ is the same as the $E(\rho^2)$ of Abramowitz and Stegun (1965), and the latter is used here. Equation 23 is the radial concentration profile across the active site for $0 < \Psi \le \Psi_c$. At Ψ_c the concentration will for the first time be zero at the site center. Then from Eq. 23,

$$0 = c_0 - 2c_0\Psi_c E(0)/\pi, \tag{24}$$

where the value $E(0) = \pi/2$ for the elliptic integral (Abramowitz and Stegun, 1965), and the critical value of Ψ is unity,

$$\Psi_c = 1. \tag{25}$$

In the second scenario, $\Psi_c < \Psi < \Psi_\infty$, given by Eqs. 11a–11c, the dimensionless rate Ψ is sufficiently large that, within a circular subregion of radius $\rho_0 < 1$ (or $r_0 < a$) about the site center, diffusion limitation controls the reaction rate. As the integral (Eq. 17) for u must now be introduced into three boundary equations (Eqs. 10, 11b, 11c), triple-integral equations must be simultaneously solved to generate $A(\xi)$ and R. Less is known about solution techniques for triple-integral equations; however, this particular problem can be simplified to a dual-integral equation problem.

The concentration is split into a sum of two parts:

$$c = c_1 + c_2, \tag{26a}$$

where

$$c_1 = c_0(1 + u_1) \tag{26b}$$

and

$$c_2 = c_0 u_2. \tag{26c}$$

The first part, c_1 and u_1, will continue to satisfy Eqs. 6–8 of the previous section, and in particular the surface boundary conditions expressed in Eqs. 9 and 10b:

$$\frac{\partial u_1}{\partial \zeta} = 0, \qquad 1 < \rho < \infty, \qquad \zeta = 0 \tag{27}$$

and

$$\frac{\partial u_1}{\partial \zeta} = \Psi, \qquad 0 < \rho < 1, \qquad \zeta = 0. \tag{28}$$

The function u_1 is then the integral (Eq. 17), with the Hankel coefficient $A_1(\xi)$ given by Eqs. 20 and 21, and the concentration contribution c_1 is Eq. 23 extended to the case $\Psi_c < \Psi < \Psi_\infty$. The second part, c_2 and u_2, also has the form of the integral (Eq. 17), with Hankel coefficient $A_2(\xi)$ selected to satisfy the conditions:

$$\frac{\partial u_2}{\partial \zeta} = 0, \qquad \rho_0 < \rho < \infty, \qquad \zeta = 0, \tag{29}$$

along with the vanishing of the dimensionless surface concentration within the region of diffusion control

$$c_1 + c_2 = c_0(1 + u_1 + u_2) = 0, \qquad 0 < \rho < \rho_0, \qquad \zeta = 0. \tag{30}$$

The $u(= u_1 + u_2)$ sum meets the conditions expressed by Eqs. 5–9, while the net surface kinetics of the sum is equivalent to those given by Eqs. 11b, 11c, and the scenario in Eq. 11a.

For the case $\Psi > \Psi_c$, the concentration equation (Eq. 23) applies only for c_1:

$$c_1 = c_0 - 2c_0\Psi E(\rho^2)/\pi, \tag{31}$$

and the value of c_1 crosses from positive to negative at the radial coordinate value ρ_0,

$$E(\rho_0^2) = \pi/(2\Psi). \tag{32}$$

This equation provides the ρ_0 defined, and used in Eqs. 11a–11c for Ψ greater than Ψ_c but less than Ψ_∞. Further, note that the zero-concentration circular region, and its radius ρ_0, moves out from $\rho_0 = 0$ when $\Psi_c = 1$ to the edge of the active site at the maximum value of Ψ for the scenario in Eq. 11a of

$$\Psi_\infty = \pi/2, \qquad \rho_0 = 1. \tag{33}$$

For $\Psi \ge \Psi_\infty$ the entire site is diffusion limited, its reaction current R_∞ is given by Eq. 1, and the solution is already known (Tranter, 1966) to be given by Eqs. 5 and 17, with the Hankel coefficient $A_\infty(\xi)$

$$A_\infty(\xi) \equiv -(2/\pi)\xi^{-2}\sin\xi, \Psi \ge \Psi_\infty. \tag{34}$$

To understand the second portion of the concentration c_2 (or $c_0 u_2$) when $\Psi_c < \Psi < \Psi_\infty$, it is helpful to consider the equivalent thermal conduction problem. Within the site subcircle of radius $\rho_0 < 1$, the function c_1 (or $c_0(1 + u_1)$) from Eq. 31 is negative, with a zero value at the edge ρ_0. The boundary condition (Eq. 30) requires that $u_2(= -1 - u_1)$ match the corresponding positive temperature distribution within the ρ_0 circle and vanish at the edge. The condition in Eq. 29 requires perfect insulation elsewhere in the infinite plane, and the temperature falls to zero far from the site center. Hence $c_1 + c_2$ is zero within the circle and on its circumference, the radial locus ρ_0, and both c_1 and c_2 are positive immediately outside the subcircle. But c_1 will increase and c_2 will decrease moving away from the ρ_0 circle. The sum of the c_1 and c_2 contributions, Eq. 26, has the necessary physical characteristics of the solution we seek.

Equation 17, valid for u_2 and its Hankel coefficient $A_2(\xi)$, when substituted into the surface boundary conditions (Eqs. 29 and 30), along with the Hankel form (Eq. 22) of Eq. 31, generates dual integral equations, respectively,

$$\int_0^\infty d\xi \left[-\xi^2 A_2(\xi) \right] J_0(\rho\xi) = 0, \quad \rho_0 < \rho < \infty, \tag{35}$$

and

$$\int_0^\infty d\xi \xi^{-1}\left[-\xi^2 A_2(\xi)+\Psi J_1(\xi)\right] J_0(\rho\xi)=1, \quad 0<\rho<\rho_0. \tag{36}$$

Tranter (1966) has presented a solution method for dual integral equations based on Jacobi's polynomial $P_m^{(0,-1/2)}$, and a one-to-one-relationship between $P_m^{(0,-1/2)}$ and the Bessel functions of order $2m+1/2$. To proceed with this method and recast Eqs. 35 and 36 into the appropriate forms, we transform to the independent variables ν and μ:

$$\rho_0 \nu = \rho \tag{37a}$$

and

$$\mu = \rho_0 \xi. \tag{37b}$$

The resulting integral forms are

$$\int_0^\infty d\mu f_2(\mu) J_0(\nu\mu)=0, \quad 1<\nu<\infty \tag{38}$$

and

$$\int_0^\infty d\mu\mu^{-1}\left[f_2(\mu)+\Psi J_1(\mu/\rho_0)\right] J_0(\nu\mu)=1, \quad 0<\nu<1, \tag{39}$$

where

$$f_2(\mu) = -(\mu/\rho_0)^2 A_2(\mu/\rho_0). \tag{40}$$

The positive constant ρ_0 is given by Eq. 32 for any Ψ between Ψ_c and Ψ_∞.

To proceed further Tranter (1966) introduces a relationship between sets of Jacobi's polynomials $P_m^{(0,-1/2)}$ and Bessel functions

$$P_m^{(0,-1/2)}(1-2\nu^2) = \frac{\sqrt{1-\nu^2}}{\sqrt{2}} \frac{\Gamma(m+1/2)}{\Gamma(m+1)} \times \int_0^\infty d\mu\mu^{1/2} J_{2m+1/2}(\mu) J_0(\nu\mu), \tag{41}$$

where m is a nonnegative integer. Note that the integral vanishes (Tranter, 1966) when $1<\nu<\infty$, or

$$P_m^{(0,-1/2)}(1-2\nu^2)=0, \quad 1<\nu<\infty, \tag{42}$$

then the inverse Hankel transform of Eq. 41 along with Eq. 42 gives the Bessel function of order 2m+1/2

$$\mu^{-1/2} J_{2m+1/2}(\mu) = \frac{\Gamma(m+1)}{\Gamma(m+1/2)}\sqrt{2}\int_0^1 d\nu\nu(1-\nu^2)^{-1/2} \times P_m^{(0,-1/2)}(1-2\nu^2) J_0(\nu\mu). \tag{43}$$

The function f_2 is expressed as an infinite series of Bessel functions

$$f_2(\mu) = \mu^{1/2} \sum_{m=0}^\infty a_m J_{2m+1/2}(\mu) \tag{44}$$

The constants a_m are determined by substitution into Eqs. 38 and 39:

$$\sum_{m=0}^\infty a_m \int_0^\infty d\mu\mu^{1/2} J_{2m+1/2}(\mu) J_0(\nu\mu)=0, \quad 1<\nu<\infty \tag{45}$$

and

$$\sum_{m=0}^\infty a_m \int_0^\infty d\mu\mu^{-1/2} J_{2m+1/2}(\mu) J_0(\nu\mu) + \Psi\int_0^\infty d\mu\mu^{-1} J_1(\mu/\rho_0) J_0(\nu\mu)=1. \tag{46}$$

Equations 41 and 42 guarantee that the surface boundary condition (Eq. 45) is always satisfied.

The second integral boundary condition (Eq. 46) is multiplied by

$$\sqrt{2}\,\nu(1-\nu^2)^{-1/2}\Gamma(n+1) P_n^{(0,-1/2)}(1-2\nu^2)/\Gamma(n+1/2),$$

where n is a nonnegative integer, and integrated over ν from 0 to 1. The integral relationship (Eq. 43) is applied to both integrals that result on the lefthand-side, to obtain

$$\sum_{m=0}^\infty a_m \int_0^\infty d\mu\mu^{-1} J_{2m+1/2}(\mu) J_{2n+1/2}(\mu) + \Psi\int_0^\infty d\mu\mu^{-3/2} J_1(\mu/\rho_0) J_{2n+1/2}(\mu) = \sqrt{2}\,\frac{\Gamma(n+1)}{\Gamma(n+1/2)}\int_0^1 d\nu\nu(1-\nu^2)^{-1/2} P_n^{(0,-1/2)}(1-2\nu^2). \tag{47}$$

The integral within the summation in Eq. 47, the orthogonality integral for the set of functions $J_{2n+1/2}(\mu)$, is given in Watson (1966),

$$\int_0^\infty d\mu\mu^{-1} J_{2m+1/2}(\mu) J_{2n+1/2}(\mu) = \delta_{m,n}(4n+1)^{-1} \tag{48}$$

in terms of the Kronecker delta function $\delta_{m,n}$.

The term on the righthand-side of Eq. 47 contains the orthogonality integral for Jacobi polynomials in terms of the Gamma function Γ,

$$\int_0^1 d\nu\nu(1-\nu^2)^{-1/2} P_n^{(0,-1/2)}(1-2\nu^2) P_m^{(0,-1/2)}(1-2\nu^2) = \frac{\delta_{m,n}}{(4n+1)}. \tag{49}$$

Noting that the zeroth-order Jacobi polynomial is unity

$$P_0^{(0,-1/2)}(1-2\nu^2)=1, \tag{50}$$

and using the orthogonality integrals (Eqs. 48 and 49), we can generate from Eq. 47 the expression for a_n,

$$a_n=(4n+1)\left[(2/\pi)^{1/2}\delta_{n,0}-\Psi H_n\right]. \tag{51}$$

The integral,

$$H_n=\int_0^\infty d\mu\mu^{-3/2}J_1(\mu/\rho_0)\,J_{2n+1/2}(\mu), \tag{52}$$

is listed by Bateman (1954) in terms of the hypergeometric function ${}_2F_1$

$$H_n=\frac{\Gamma(n+1/2)\,\rho_0^{2n}}{2^{3/2}\Gamma(2n+3/2)\Gamma(-n+3/2)} \times {}_2F_1\left(n+1/2,\ n-1/2;\ 2n+3/2;\rho_0{}^2\right). \tag{53}$$

The site reaction current R for the scenario in Eq. 11a, when $\Psi_c<\Psi<\Psi_\infty$, is diffusion-controlled by Eq. 11c from the site center to ρ_0, and zeroth order by Eq. 11b with a dimensionless reaction rate Ψ per unit area from ρ_0 to the site edge at $\rho=1$. Under these conditions, Eq. 13, made dimensionless by R_∞ the diffusion control limit (Eq. 1) of R, becomes

$$\frac{R}{R_\infty}=\frac{\pi}{2}\int_0^{\rho_0}d\rho\rho\left.\frac{\partial u}{\partial\zeta}\right|_{\zeta=0}+\frac{\pi}{4}\Psi\left(1-\rho_0^2\right). \tag{54}$$

The split (Eqs. 26a–26c) of the dimensionless concentration (Eq. 6), $u=u_1+u_2$, along with the surface reaction condition (Eq. 28) for u_1, allows Eq. 54 to be expressed solely in terms of the gradient $\partial u_2/\partial\zeta$ evaluated at the surface $\zeta=0$:

$$\frac{R}{R_\infty}=\frac{\pi}{4}\Psi+\frac{\pi}{2}\int_0^{\rho_0}d\rho\rho\left.\frac{\partial u_2}{\partial\zeta}\right|_{\zeta=0}. \tag{55}$$

Using the Hankel transform expression (Eq. 17) to write u_2 of Eq. 55 in terms of $A_2(\xi)$,

$$\frac{R}{R_\infty}=\frac{\pi}{4}\Psi-\frac{\pi}{2}\int_0^{\rho_0}d\rho\rho\int_0^\infty d\xi\xi^2A_2(\xi)\,J_0(\rho\xi), \tag{56}$$

interchanging the order of the integrations in Eq. 56, and changing the variables in the radial ρ integration to $t=\xi\rho$, we can integrate over t and express the reaction-site current in terms of the first-order Bessel function $J_1(\rho_0\xi)$

$$\frac{R}{R_\infty}=\frac{\pi}{4}\Psi-\frac{\pi}{2}\int_0^\infty d\xi A_2(\xi)\rho_0\xi J_1(\rho_0\xi). \tag{57}$$

The well-known integral relationship (Abramowitz and Stegun, 1965) between the t integration of $t\,J_0(t)$ from 0 to $\rho_0\xi$ and the product $\rho_0\xi J_1(\rho_0\xi)$ has been used to derive Eq. 57.

The variables μ and f_2, respectively, from Eqs. 37b and 40, as well as the Bessel function expansion (Eq. 44) are substituted into Eq. 57:

$$\frac{R}{R_\infty}=\frac{\pi}{4}\Psi+\frac{\pi}{2}\rho_0\sum_{m=0}^\infty a_m\int_0^\infty d\mu\mu^{-1/2}J_{2m+1/2}(\mu)\,J_1(\mu). \tag{58}$$

Once again, the integral of the Bessel function product in Eq. 58 can be found in Watson's treatise (1996), and expressed in terms of Gamma functions,

$$\frac{R}{R_\infty}=\frac{\pi}{4}\Psi+\left(\frac{\pi}{2}\right)^{3/2}\rho_0\sum_{m=0}^\infty a_m\frac{\Gamma(1+m)}{\Gamma(1-m)\Gamma(m+3/2)\Gamma(m+1/2)}. \tag{59}$$

The denominator in the terms of the sum in Eq. 59 contains the Gamma function $\Gamma(1-m)$, which will be infinite for all but $m=0$, and truncates the series at the first term. With Eqs. 51–53 for a_m, the dimensionless site-reaction current can be expressed directly in terms of the hypergeometric function ${}_2F_1$

$$\frac{R}{R_\infty}=\frac{\pi}{4}\Psi+\rho_0\left[1-\Psi{}_2F_1\left(1/2,-1/2;3/2;\rho_0^2\right)\right]. \tag{60a}$$

The value of this hypergeometric function can be readily obtained (Abramowitz and Stegun, 1965),

$${}_2F_1\left(1/2,-1/2;3/2;\rho_0^2\right)=1/2\left[\left(1-\rho_0^2\right)^{1/2}+\rho_0^{-1}\arcsin\rho_0\right]. \tag{60b}$$

Along with Eq. 34 for the ρ_0 values as a function for Ψ, Eqs. 60a and 60b provide the dimensionless site reaction current in the intermediate kinetic range, that is, $\Psi_c<\Psi<\Psi_\infty$.

Discussion and Conclusions

A brief summary of the receptor-site reaction current behavior for the zeroth-order, specific binding kinetics model following the scenario of Eqs. 10a–13 requires that one of three physical situations will exist at the site.

$0<\Psi\le 1$

In the slower reaction rate region, the local site surface reaction has no diffusion control. The dimensionless specific reaction rate $\Psi\ [=a\sigma/(c_0D)]$ lies above zero and is less than or equal to one. The dimensionless site reaction-rate current from Eqs. 1 and 10c is

$$R_0/R_\infty=\pi\Psi/4. \tag{61}$$

The nutrient or ligand concentration drops from the concentration c_0 far from the active site to a minimum value at the

receptor center of

$$c(\zeta = 0,\ \rho = 0) = c_0(1 - \Psi). \tag{62}$$

$1 < \Psi < \pi/2$

For intermediate reaction rates, within the circular region from the site center $\rho = 0$ to the dimensionless radial coordinate ρ_0, the site surface concentration is zero and the local surface reaction is diffusion controlled. From ρ_0 to the receptor site edge at $\rho = 1$, zeroth-order kinetics holds. The value of the dimensionless radius locus ρ_0 for transition from diffusion control to zeroth-order kinetic comes from the elliptic integral

$$E(\rho_0^2) = \pi/(2\Psi). \tag{32}$$

The dimensionless reaction rate for the intermediate kinetics $1 < \Psi < \pi/2$ is determined by a combination of Eqs. 60a and 60b

$$\frac{R}{R_\infty} = \frac{\pi\Psi}{4} + \rho_0\left\{1 - \frac{\Psi}{2}\left[\left(1 - \rho_0^2\right)^{1/2} + \rho_0^{-1}\arcsin\rho_0\right]\right\}. \tag{63}$$

For any Ψ kinetics rate ρ_0 is calculated from Eq. 32, and the ratio R/R_∞ is only a function of Ψ.

$\pi/2 \le \Psi < \infty$

That the case of total site diffusion control gives the reaction current R_∞ of Eq. 1 has already been shown (Berg, 1993).

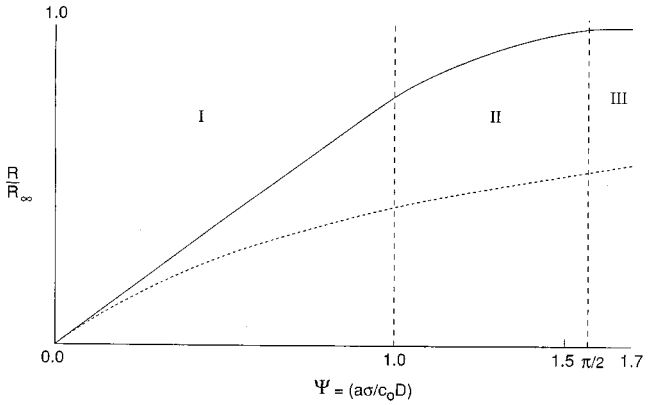

Figure 1. Ratio of the site reaction current R to the diffusion-controlled site-reaction current limit R_∞ is plotted as a solid curve vs. the dimensionless zeroth-order reaction rate $\Psi[= a\sigma/(c_0 D)]$.

Also shown are the Ψ regions; I—zeroth-order kinetics completely across the site; II—diffusion-controlled reaction within an inner site region of radius $\rho_0 < 1$ with zeroth-order site-reaction kinetics outside the inner circle; and III—diffusion-controlled kinetics across the full site. The R/R_∞ approximation, generated by the series addition of the diffusion-controlled and reaction-controlled site-reaction current limits, is shown as the dashed curve.

But the reasonable kinetic range of Ψ in which R_∞ is a valid site reaction current is new.

The dimensionless site reaction currents listed earlier, Eqs. 61 and 63, are shown in Figure 1, plotted as a solid line vs. the dimensionless specific reaction rate Ψ per unit area. The three kinetics regions—I lower. II intermediate, and III diffusion-controlled rates—are indicated with the two vertical dotted lines. They provide the various reaction kinetic ranges and expected behavior in terms of molecular diffusion and intrinsic kinetic constants. The diffusion-controlled region gives an indication of the specific reaction rates, ligand diffusion coefficients, and applied concentrations necessary, in order that the assumption of a diffusion-controlled receptor, as was done by Purcell and Berg (1997), Berg (1993), Zwanzig (1990) and others, is appropriate.

The curves and kinetics regions of Figure 1 can be used along with state-of-the-art kinetic and transport coefficients to obtain some idea of the influence of diffusion on growth-factor internalization, nutrient uptake, the desensitization of signaling receptors and other cellular ligand receptor processes. Schwartz (1990) has given a range for the kinetic constant for internalization ($\pi a^2\sigma$) from 0.12 to 0.46 min^{-1} per site per internalized ligand–receptor complex. Lauffenburger and Linderman (1993) suggest a diffusion coefficient range of 10^{-5} to 10^{-7} cm^2/s, and a ligand diffusivity of 10^{-6} cm^2/s seems reasonable. Also 1 nm is usually used for the active site radius. For a ligand concentration of 5×10^{-9} molar, which is in the zeroth-order range for the growth-factor data (Wiley and Cunningham, 1981), the Ψ range calculated from Eq. 5 runs from 0.002 to 0.008, with little site diffusion resistance for instances of extracellular free solution. On the other hand, microorganisims are often found in biofilms or bioflocs. Bailey and Ollis (1986), in discussing this additional diffusive resistance, state the O_2 diffusion coefficient in microbial aggregates decreases from the free-solution, pure-water value with increased aggregate lifetime from 5:1 to 20:1. Similar increases in diffusive resistance are observed for glucose, and for much larger polypeptides at least this amount of resistance is possible. In biofilms and flocs, Ψ values as large as 0.16 do generate significant concentration profiles about the individual site, but the zeroth-order site kinetics is insensitive to these concentration differences, strictly requiring Ψ to be above unity before they are recognized. However, the general Michaelis-Menten kinetics should exhibit site diffusion resistance effects under similar conditions in a film or floc.

While internalization processes are often found near neutral pH, ligand–receptor association and across-wall transport can occur at other pH conditions, for example, inside cellular vesicles. Koren and Hammes (1976) have done experiments for protein interactions at lower pH values (pH values of 4.3 and 3.7), where significant charges develop at the macromolecular active sites. It has been known for some time (Alberty and Hammes, 1958; Hammes and Alberty, 1959) that charge effects can play an important role in molecular biological transport processes, and Koren and Hammes (1976) have estimated effective diffusion coefficient reductions (10^{-2} and 10^{-3}, respectively, for the pH values of their experments) that suggest at lower pH, diffusion control can exist even in free solution.

Results of the customary approximate procedure (Lauffenburger and Linderman, 1993) of adding the chemical- and

diffusion-limiting net site reaction rates in series, Eqs. 4 and 5, are also given in Figure 1 as a dashed curve. In the case of zeroth-order kinetics and a circular active site, series addition to generate net site kinetics is not accurate. The resulting R/R_∞ values are off by a factor of 2, when the specific dimensionless site kinetics $\Psi = \Psi_\infty = \pi/2$.

The simple forms of the receptor site reaction (Eqs. 1, 61, and 63) provide a useful model for cell-nutrient uptake, growth-factor internalization, and signaling receptor desensitization. The site reaction curve in Figure 1 that results, provides the full form of the exact solution of the ligand-diffusion−Michaeles-Menten site kinetics problem near the limit of vanishing denominator constant-bulk ligand concentration ratio, that is, $K/c_0 \to 0$. The curve must include all the biophysics that are the basis of the full Michaeles-Menten kinetics-binding dissociation, and internalization. In particular, the interesting region between the constant site kinetics and full diffusion control ($1 < \Psi < \pi/2$ in Figure 1) must be a rigorous part of the true ligand-diffusion−Michaeles-Menten site reaction behavior in the neighborhood of large site binding rates.

Notation

K = denominator constant in Michaelis-Menter kinetics
r_m = specific site kinetics per unit area
r_0 = radius of diffusion-controlled region of site
Γ = Gamma function
σ = zeroth-order reaction rate per unit site area

Literature Cited

Abramowitz, M., and I. A. Stegun, *Handbook of Mathematical Functions*, National Bureau of Standards, Washington, DC (1965).

Alberty, R. A., and G. G. Hammes, ''Application of the Theory of Diffusion-Controlled Reactions to Enzyme Kinetics,'' *J. Phys. Chem.*, **62**, 154 (1958).

Bailey, J. E., and D. F. Ollis, *Biochemical Engineering Fundamentals*, McGraw-Hill, New York (1986).

Bateman, H., *Tables of Integral Transforms*, McGraw-Hill, New York (1954).

Berg, H. C., *Random Walks in Biology*, Princeton Univ. Press, Princeton, NJ (1993).

Berg, H. C., and E. M. Purcell, ''Physics of Chemorception,'' *Biophys. J.*, **20**, 193 (1977).

Berg, H. C., and P. H. von Hippel, ''Diffusion-Controlled Macromolecular Interactions,'' *Chem. Annu. Rev. Biophys.*, **14**, 131 (1985).

Hammes, G. G., and R. A. Alberty, ''The Influence of Net Protein Charge on the Rate of Formation of Enzyme-Substrate Complexes,'' *J. Phys. Chem.*, **63**, 274 (1959).

Hoffman, J. F., J. J. Linderman, and G. M. Omann, ''Receptor Up-Regulation, Internalization and Interconverting Receptor Sites,'' *J. Biol. Chem.*, **271**, 18394 (1996).

Koren, R., and G. G. Hammes, ''A Kinetic Study of Protein-Protein Interactions,'' *Biochemistry*, **15**, 1165 (1976).

Lauffenburger, D. A., and J. J. Linderman, *Receptors-Models for Binding, Trafficking, and Signalling*, Oxford Univ. Press, Oxford (1993).

Maalmi, M., A. Varma, and W. Strieder, ''The Sharp Interface Model: Zeroth Order Reaction with Volume Change,'' *Ind. Eng. Chem. Res.*, **34**, 1114 (1995).

Northrup, S. H., ''Diffusion Controlled Ligand Binding to Multiple Competing Cell-Bound Receptors,'' *J. Phys. Chem.*, **92**, 5847 (1998).

Schwartz, A. L., ''Cell Biology of Intracellular Protein Trafficking,'' *Annu. Rev. Immunol.*, **8**, 195 (1990).

Strieder, W., ''Chemoreceptor Diffusion and Reaction: First Order Kinetics,'' *Chem. Eng. Sci.*. **55**, 2579 (2000).

Tranter, C. J., *Integral Transforms in Mathematical Physics*, Butler and Tanner, London (1966).

Watson, G. M., *Theory of Bessel Functions*, Cambridge University Press, Cambridge (1966).

Wiley, S. H., and D. D. Cunningham, ''A Steady State Model for Analyzing the Cellular Binding Internalization and Degradation of Polypeptide Ligands,'' *Cell*, **25**, 433 (1981).

Zwanzig, R., ''Diffusion Controlled Ligand Binding to Spheres Partially Covered by Receptors: An Effective Medium Approach,'' *Proc. Natl. Acad. Sci. USA*, **87**, 5856 (1990).

Manuscript received June 30, 1999, and revision received Apr. 26, 2000.